NUMERICAL ANALYSIS OF THE INFLUENCE OF THE DIMENSIONS OF SPIRES IN AN ATMOSPHERIC BOUNDARY LAYER WIND TUNNEL

Luiz Fernando Ribeiro Ledo
Júlio César Xavier Ribeiro
Sérgio de Morais Hanriot
Cristiana Brasil Maia
Pontifícia Universidade Católica de Minas Gerais, Av. Dom José Gaspar, 500 – Coração Eucarístico, 30535-901, Belo Horizonte, Minas Gerais, Brasil
lribeiroledo@yahoo.com.br, jcxrjulio@gmail.com, hanriot@pucminas.br, cristiana@pucminas.br

Abstract. *Wind tunnels used to simulate external fluid flows usually present large dimensions for the complete development of the fluid flow and the consequent possibility to suitably represent the atmospheric boundary layer. Because of the difficulty to build and operate large wind tunnels, spires are used to accelerate the boundary layer development. Spires are cut and folded devices of triangular plates, positioned in the test section inlet. In this work, a numerical model was developed to analyze the influence of the thickness and the size of the spires in the behavior of the fluid flow. The dimensions of the wind tunnel used as reference are those of the Plint & Patners LDD Whokinghan Bershire England wind tunnel. It has a squared test section, with 460 mm of edge and 1200 mm of length. It also uses a channel that extends the test section 1200 mm, with an internal width of 410 mm. The main dimensions of the spires were varied: the thickness of the plate with spires that have been constructed, the width of the base of the reinforcement plate relative to the triangular base plate and the width of the base of the triangular plate. The commercial software ANSYS – CFX was used to simulate the steady state turbulent airflow inside the device. The development of the boundary layer and the velocity profile were evaluated in the test section, and it was observed a small influence of the spires dimensions on the development of the boundary layer and on the fluid flow behavior*.

Keywords: *ANSYS CFX, CFD, Atmospheric Boundary Layer Wind Tunnel, Spires*

1. INTRODUCTION

The simulation of atmospheric flows in wind tunnels can be used to study topographic effects and the turbulence generation from the surface in objects. The measurements on wind tunnels depend on its dimensions, the dimensions of the simulated environment, the flow speed, the turbulent properties, as well as on the characteristics of the measurement instruments used.

Due to the vast use of wind tunnel models simulations, one can consider that a well conducted wind tunnel simulation in a scale model can be effectively applied to a full-scale prototype. Cook (1978) studied some methods to determine the model scale. The author established and determined some key parameters; then presented the influence of these parameters on the simulations results. The main conclusions were that the linear scale of any building model should be matched to the scale factor calculated; otherwise the scales of the simulated atmospheric turbulence and the building-generated turbulence will not match. In that event, the scaled dynamic response of the model in load or in deflection will not be correct.

On the majority of wind tunnels, the test section is not long enough for the study of a fully developed boundary layer. Due to the need of a longer test section and the difficulty to build a wind tunnel with the required dimensions, some devices can be used to help achieve the desired conditions. Two of these devices are spires and channel.

Spires are devices made of folded triangular or tetrahedral plates positioned at the beginning of the test section with the goal to simulate natural winds. Channels are utilized to create a longer test section, making the studied area bigger and easier to obtain a fully developed atmospheric boundary layer. Some other devices like a serrated fence and regular or varying holes thickener can also be found in the literature (Sargison et al., 2004).

There are in the literature several papers regarding atmospheric boundary layer wind tunnels. Spires are used in combination with the ground roughness to produce large scale turbulence intensity data compatible with the Planetary Boundary Layer. Counihan (1969) presented an experimental evaluation of various types of turbulence generators leading to the adoption of an elliptical wedge system and a castellated barrier. The length of the test section has to be four to five times the boundary layer height. Irwin (1981) presented a study of the equations used to build spires for use in planetary boundary layer simulations. Barbosa et al. (2002) proposed a method for the production of thick boundary layer in small wind tunnels using fabrics, elliptical, wedge and cylindrical rod generators. Loredo-Souza et al. (2004) presented a study of simulation techniques of atmospheric boundary layer in wind tunnels, controlling the shear stress and the shear rate by the roughness of the terrain.

The use of Computational Fluid Dynamics (CFD) techniques to evaluate the behavior of the airflow is also a vastly discussed subject in the literature. Blocken et al. (2007) presented a discussion on the importance of precision found in CFD studies that may be seriously compromised when the wall roughness function is changed. The problems typically manifest as involuntary gradients in the mean velocity and turbulence profiles, being blamed by certain discrepancies found in some CFD simulations. At their work, the authors discuss in details the problem and its negative consequences with suggestions for possible improvements to the simulations. There are some other issues regarding CFD, like the simulation of the directional variability of the wind and the determination of the effect of large-scale, transverse velocity fluctuations; the determination of the effect of the length scales of the turbulence in relation to building size; the elucidation of the role of small scale fluctuations, specifically in the inertial subrange of the turbulence spectrum, and their effect for example on the magnitude of peak pressures; and the determination of any associated scale effects (Farell et al., 1999).

This paper presents a numerical analysis on the influence of the dimensions of triangular spires positioned at the entrance of the test section of a wind tunnel. The parameters evaluated were the lengths of the reinforcement and the triangular base and the spire plates' thickness. Other researchers have presented studies on the current studied tunnel. Roballo and others (2009) presented an experimental study of the atmospheric flow at the Alcantara Launch Center through a simulation in a wind tunnel, and Pires and others (2010) presented the measurement of the atmospheric flow in the wind tunnel using hot wire anemometers and the Particle Image Velocimetry technique (PIV).

2. NUNERICAL METHODOLOGY

The governing equations of the problem are the mass and momentum conservation equations and the transport equations for the turbulent properties. ANSYS/CFX 14.5 was used to solve the governing equations.

- Mass conservation equation (White, 2006):

$$\frac{\partial}{\partial t}\rho + \nabla \bullet \left(\rho \overline{\mathbf{U}}\right) = 0 \tag{1}$$

- Momentum conservation equation (White, 2006):

$$\frac{D\left(\rho \overline{\mathbf{U}}\right)}{Dt} = \rho \mathbf{g} - \nabla \overline{p} + \nabla \bullet \tau_{ij} \tag{2}$$

Where the Reynolds stress tensor is given by (White, 2006):

$$\tau_{ij} = \mu\left(\frac{\partial u_i}{\partial x_j} + \frac{\partial u_j}{\partial x_i}\right) - \rho \overline{u_i' u_j'} \tag{3}$$

The K-ω SST model was used to evaluate the turbulent properties (Veersteg and Malalasekera, 2007). For the turbulent kinetic energy (K):

$$\frac{\partial(\rho K)}{\partial t} + \nabla \bullet \left(\rho K \mathbf{U}\right) = \nabla \bullet \left[\left(\mu + \frac{\mu_t}{\sigma_K}\right) \cdot \nabla(K)\right] + \left(2\rho S_{ij} \cdot S_{ij} - \frac{2}{3}\rho K \frac{\partial U_i}{\partial x_j}\delta_{ij}\right) - \beta^* \rho K \omega \tag{4}$$

For the turbulent frequency (ω):

$$\frac{\partial(\rho\omega)}{\partial t} + \nabla \bullet \left(\rho\omega \mathbf{U}\right) = \nabla \bullet \left[\left(\mu + \frac{\mu_t}{\sigma_{\omega,1}}\right) \cdot \nabla(\omega)\right] + \gamma_2\left(2\rho S_{ij} \cdot S_{ij} - \frac{2}{3}\rho\omega \frac{\partial U_i}{\partial x_j}\delta_{ij}\right) - \beta_2 \rho \omega^2 + 2\frac{\rho}{\sigma_{\omega,2} \cdot \omega}\frac{\partial K}{\partial x_K}\frac{\partial \omega}{\partial x_K} \tag{5}$$

Where $\overline{\mathbf{U}}$ is the mean velocity vector, $\nabla \overline{p}$ is the pressure gradient ρ, μ are respectively the fluid´s density and viscosity, $\mathbf{g}$ is the gravity acceleration and t represents time.

The interpolation advection scheme was the high resolution and the numerical turbulence interpolation scheme was of First Order.

For the problem definition and boundary conditions were used experimental dada provenient from the *Plint & Partners LDD Wokingham Berkshing England* wind tunnel, its dimensions are shown in Figure 1. The first part consists of a 460mm edge and 1200mm long squared test section and the second part is a 460mm high, 410mm wide and 1200mm long channel with an open upper face. The studied conditions consist of a 0.33867 kg/s mass flow rate, obtained from experimental data found in the literature (Roballo, 2007). The resulting Reynolds number on the test section was approximately of order 10^4, characteristic of turbulent flow.

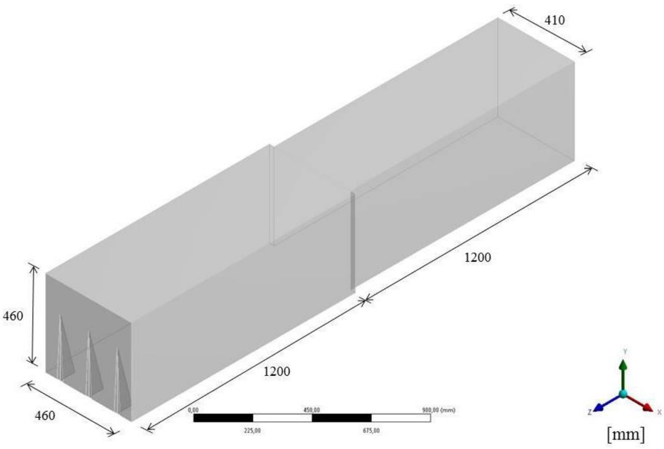

Figure 1: Computational domain and its dimensions

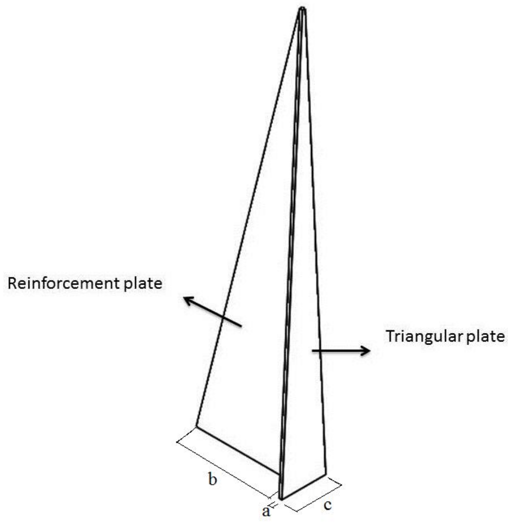

Figure 2: Spire

A schematic of a spire is shown in Fig. 2. The thickness of the plates (a) was varied between 1mm, 2mm, 3mm, and 4mm. The evaluated lengths of the reinforcement plates' base (b) were 32.6mm, 65.2mm, 97.8mm and 76.93mm, and of the triangular plates' base (c), 16.3mm, 32.6mm and 48.9mm.

The boundary conditions adopted are shown in Table 1 and Figure 3. The values were obtained from experimental data (Roballo, 2007).

Table 1: Boundary Conditions imposed on Computational Domain

Domain	**Boundary Conditions**
Inlet	Mass Flow Rate of 0.33867 kg/s
Outlet	Atmospheric Pressure
Walls	No slip condition

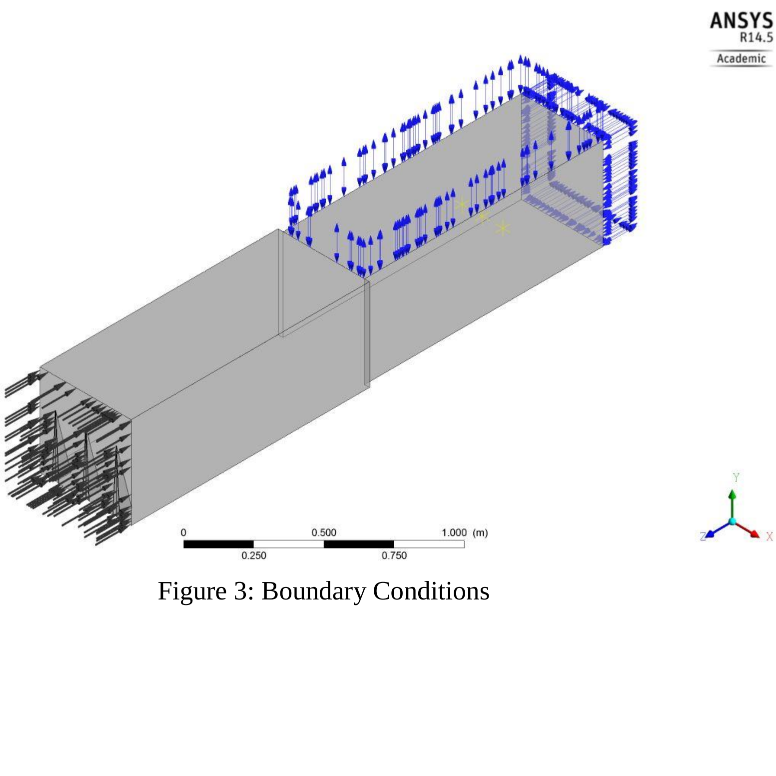

Figure 3: Boundary Conditions

The simulations were performed in a computer with 32GB RAM, Windows 64 bits, processor Intel® Xenon® E5-1660 3.30 GHz , 1TB HD.

Mesh tests were conducted, consisting of varying the maximum size of the mesh elements, with a consequent increase on the number of nodes and elements. The most refined mesh was used for analyses and dada presentation. For the mesh tests, it was set a RMS (root mean square) residual of $1.0x10^{-6}$. The average time required for the simulations with the most refined meshes was 8h41min, with an average number of nodes of 3,128,902.

The hypotheses and boundary conditions applied are:

- Air as an ideal gas;
- Steady state conditions;
- Ambient temperature: 299K;
- Atmospheric pressure: 101.3 kPa;
- Experimental mass flow rate at the inlet;
- Opening condition at the outlet and at the top of the channel;
- No slip condition at the walls.

3. RESULTS

It was defined a standard geometry for the spires, with thickness of 2mm, length of the reinforcement plate of 75.93mm and length of the triangular plate base of 32.6mm. The behavior of the airflow for this condition is shown in Fig. 4, in a horizontal plane xz positioned at 115mm from the base of the tunnel. Just upstream the spires, the velocity profile is highly non-uniform, and wakes can be seen. Consequently, the velocity profile is different when evaluated in different vertical planes.

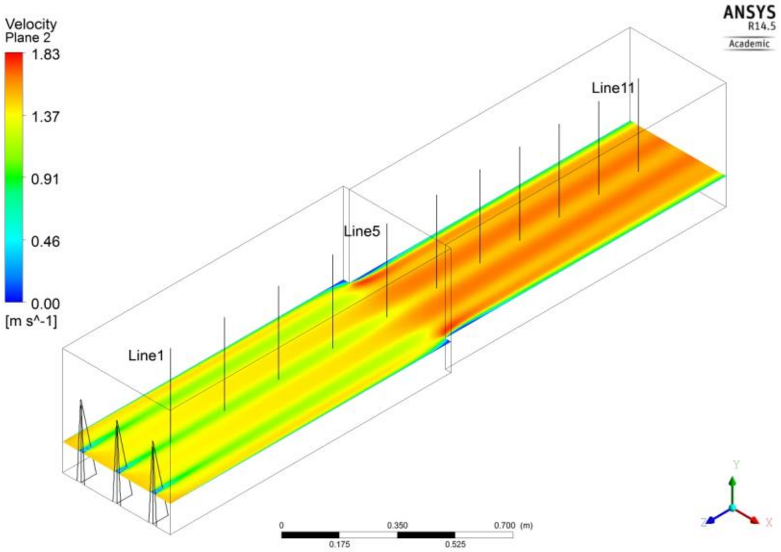

Figure 4: Velocity in a horizontal plane with standard geometry

Figure 5 represents the velocity profiles of lines 1, 5 and 11 (represented in Fig. 4) at a central vertical plane, obtained using the standard geometry spires (2mm thick spire plates, 75.93mm long reinforcement plate's base and 32.6mm long triangular plate's base). It can be noticed that the velocity is lower in line 1, due to the influence of the spires. In line 5 the velocity gets higher due to the junction between the test section and the channel; and in line 11, the velocity is the highest due to the reduction of the cross sectional area.

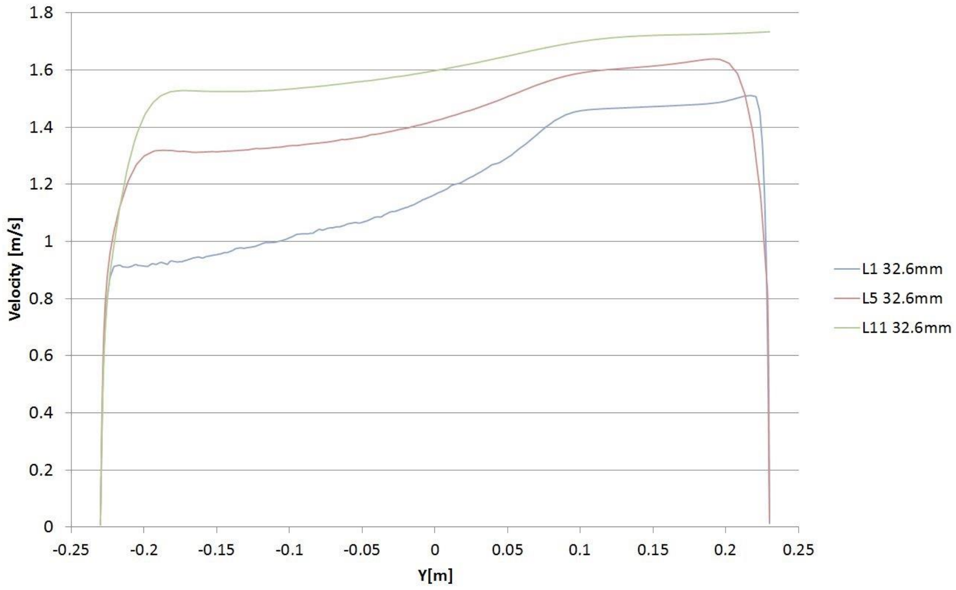

Figure 5: Velocity profile with the standard geometry

It was evaluated the influence of the thickness of the spires' plates (defined as "a" in Fig. 2) on the development of the boundary layer. The lengths of the reinforcement (b) and triangular plates (c) were the same of the standard geometry, and the thickness was varied: 1mm, 2mm, 3mm and 4mm. The velocity profiles for the thickness of the spire plates are not shown because no significant variations were found at their values.

Figure 6 shows the development of the boundary layer along the wind tunnel, for the evaluated thicknesses of the spires plates. The boundary layer thickness was determined in 11 axial positions, presented in Fig. 4 (Lines 1 to 11). The lines were presented in two vertical yz planes: the first positioned at the center of the test section (central plane), and the second, positioned in the middle of two spires (lateral plane). The boundary layer thickness increases with the thickness of the spires. However, it can be seen that the influence of the thickness of the plate on the development of the boundary layer is not significant. When comparing the development of the boundary layer on the central and lateral planes, it can be seen that the boundary layer thickness is greater on the central plane. This can be explained due to the wakes formed behind the spires. The velocity is reduced at the wakes, increasing the thickness of the boundary layer. In the lateral plane, there is lower influence of the spires. It is also observed a great reduction of the boundary layer thickness at z = 1.155 m, which corresponds to line 5. It represents the junction between the test section and the channel. A reduction of the cross sectional area causes a variation on the velocity profiles, altering the boundary layer thickness.

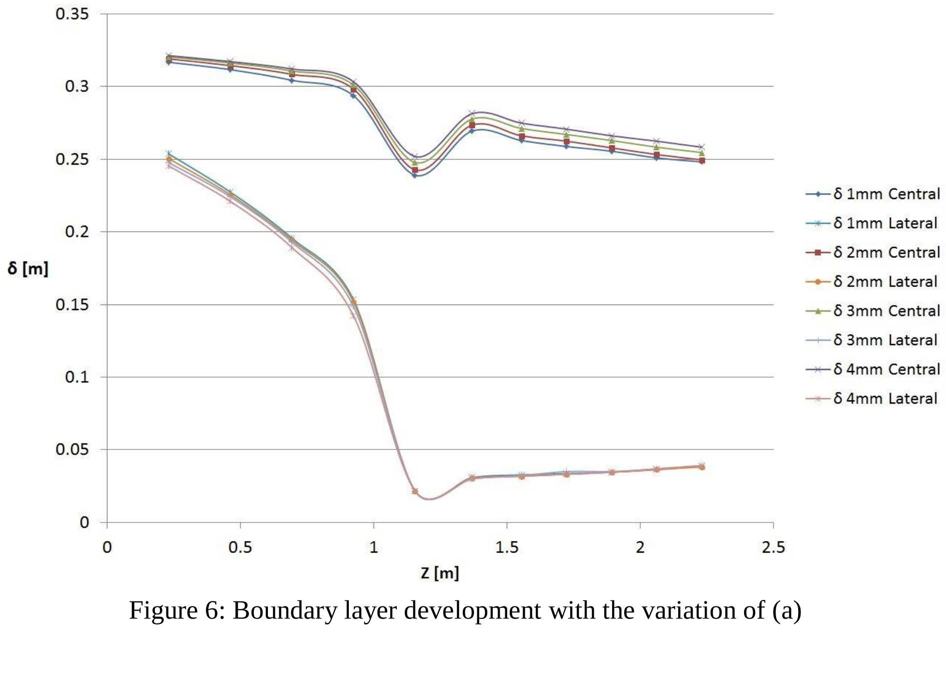

Figure 6: Boundary layer development with the variation of (a)

It was evaluated the influence of the reinforcement plates' base length (b) on the development of the boundary layer. The thickness of the spire plates and triangular plates' base length were the same of the standard geometry, and the length of the reinforcement plates' base was varied between 32.6mm, 65.2mm, 97.8mm and 76.93mm. The velocity profiles for the reinforcement plates' base are not shown because no significant variations were found at their values. Figure 7 shows the development of the boundary layer along the wind tunnel, for the evaluated length of the reinforcement plates' base, it also shows that the influence of this dimension's variation on the development of the boundary layer is not significant. This behavior was already expected. According to Irwin (1981), differences in the reinforcement base dimensions provide average differences of 1.5% in the velocity profile and development of the boundary layer.

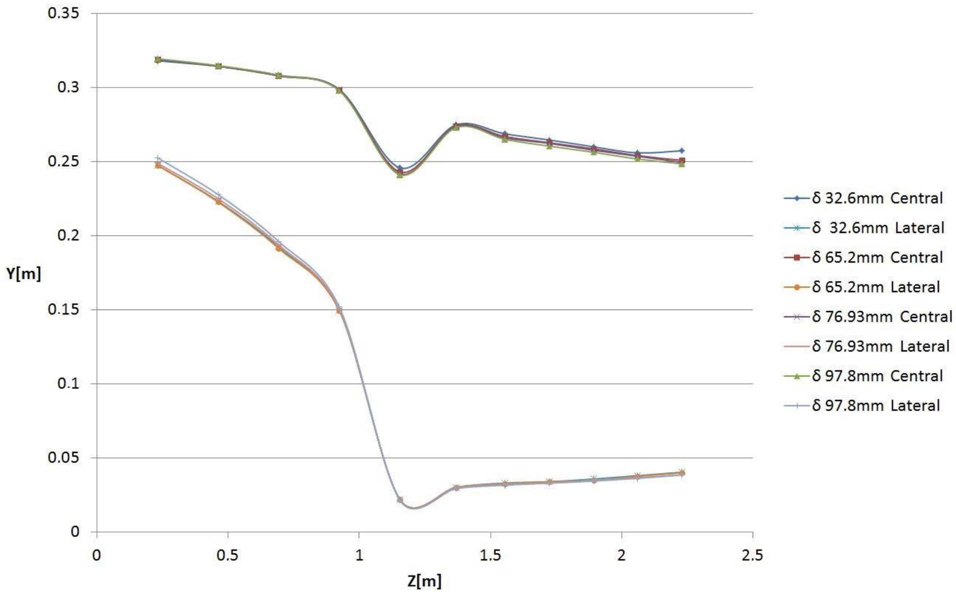

Figure 7: Boundary layer development with the variation of (b)

Figure 8 shows the development of the boundary layer along the wind tunnel with the triangular plate´s base (c) variation. The thickness of the spire plates and reinforcement plates' base length were the same of the standard geometry, and the length of the triangular plates' base was varied between 16.3mm, 32.6mm and 48.9mm.

The length of the triangular plate's base is the parameter that most affects the development of the boundary layer, especially when evaluated at the central plane. In this region, an increase of the length decreases the boundary layer thickness in the test section and increases it in the channel.

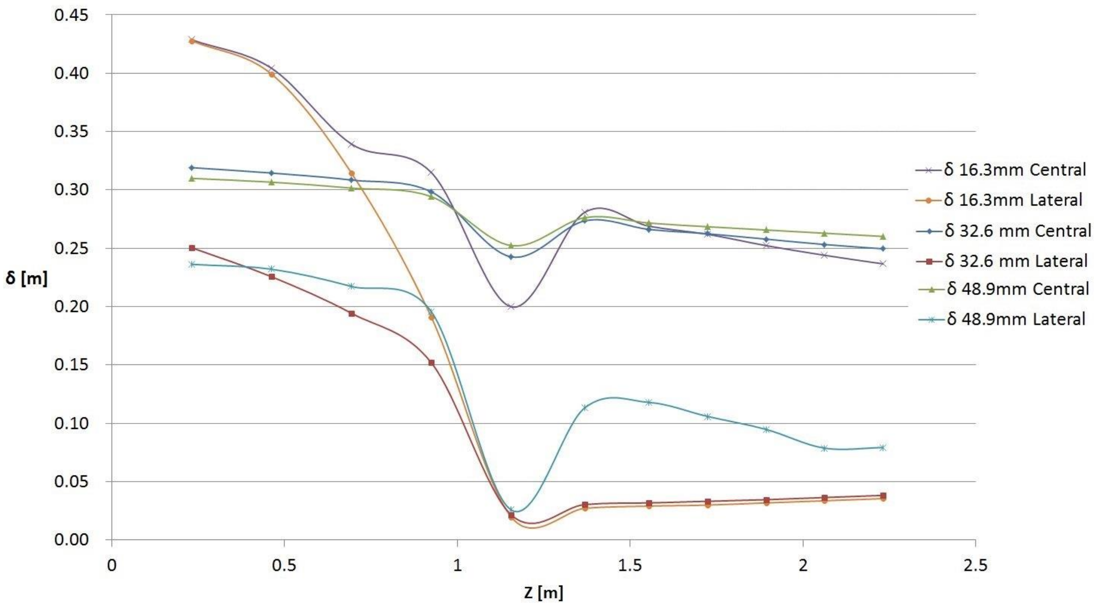

Figure 8: Boundary layer development with the variation of (c)

The value of 16.3 mm showed significant variations from the other widths evaluated, mainly at the inlet. This behavior can be explained together with the velocity fields (Figs. 9 and 10). When the sectional area of the spires decreases (16.3mm length), the average inlet velocity decreases, increasing the boundary layer thickness at this part of the tunnel.

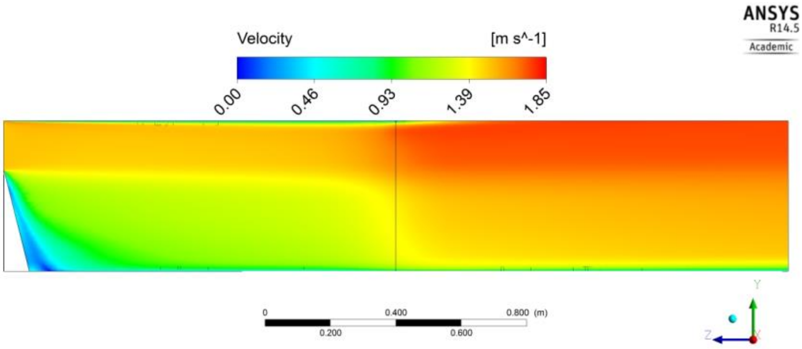

Figure 9: Velocity profile with the 48.9mm triangular plates' base

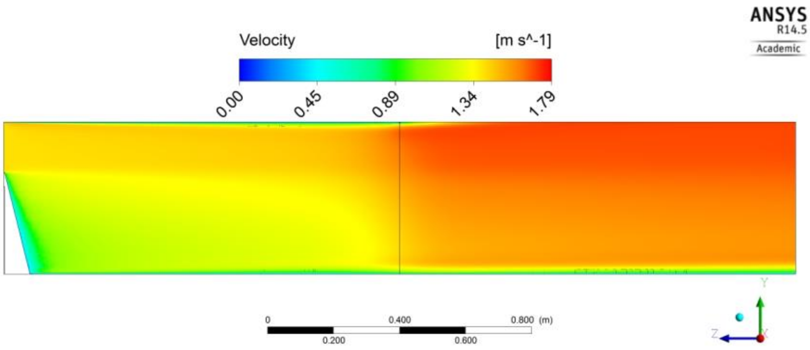

Figure 10: Velocity profile with the 16.3mm triangular plates' base

4. CONCLUSIONS

A numerical simulation of the airflow in an atmospheric boundary layer wind tunnel was performed, using the commercial software ANSYS/CFX 14.5 to solve the governing equations. The dimensions and boundary conditions were based on experimental results found in literature. To the best knowledge of the authors, only a few studies were performed regarding the influence of the dimensions of the spires on the development of the boundary layer. The parameters evaluated were the thickness of the spires' plates and the lengths of the reinforcement and triangular plates' base.

According to the results, it can be concluded that the influence of the thickness of the plates and the length of the reinforcement bases is not significant on the development of the boundary layer or in the velocity profiles. However, an increase of the length of the triangular plate increases the boundary layer thickness significantly.

The boundary layer thickness and the velocity fields were evaluated in two different vertical plates, and substantial differences were observed between them. In a wind tunnel, it is fundamental to obtain a uniform velocity profile where the body to be analyzed will be positioned. The presence of the spires increase the boundary layer thickness (as required), but provide a non-uniform velocity profile. Therefore, it is necessary to use other devices such as carpets and screens to increase the boundary layer thickness and to promote a more uniform velocity profile.

5. ACKNOWLEDGMENTS

The authors are thankful to CNPq, FAPEMIG, CAPES and PUC Minas.

6. REFERENCES

Barbosa,P. H. A., Cataldi M., Freire, A. P. S. 2002. *Wind tunnel simulation of atmospheric boundary layer flows.* J. Braz. Soc. Mech. Sci. ,vol. 24, no. 3, Rio de Janeiro.

Blocken, B., Stathopoulos, T., Carmeliet, J. 2007. *CFD simulation of the atmospheric boundary layer: wall function problems.* Atmospheric Environment 41, p. 238-252.

Cook, N.J., 1978. *Determination of the model scale factor in wind-tunnel simulations of the adiabatic atmospheric boundary layer.* Department of the Environment, Building Research Station, Garston, Warlord, United Kingdom.

Counihan, J. 1969. *An improved method of simulating an atmospheric boundary layer in a wind tunnel.* Atmospheric Environment Pergamon Press, Vol. 3, pp. 197-214.

Farell, C., Iyengar, A.K.S.1999. Experiments on the wind tunnel simulation of atmospheric boundary layers. Journal of Wind Engineering and Industrial Aerodynamics.

Irwin, H. P. A. H. 1981. *The design of spires for Wind simulation.* Journal of Wind Engineering and Industrial Aerodynamics, v.7,p.361-366.

Loredo-Souza, A. M., Schettini, E. B. C., Paluch, M. J. 2004. *Simulação da camada limite atmosférica em túnel de vento.* Associação Brasileira de Engenharia e Ciências Mecânicas.

Pires,L. B. M., Roballo, S. T., Fisch, G., Avelar, A. C., Girardi, R. da M., Gielow, R. 2010. *Atmospheric flow measurements using the PIV and HWA techniques.* J. Aerosp. Technol. Manag.. São José os Campos, Vol. 2, n. 2, p. 127-136.

Roballo, S. T. 2007. *Estudo do escoamento atmosférico no centro de lançamento de Alcântara (CLA) através de medidas de torre anemométrica e em túnel de vento.* Departamento de Meteorologia, Instituto Nacional de Pesquisas Espaciais.

Roballo, S. T., Fisch, G. 2009. *Escoamento atmosférico no Centro de Lançamento de Alcântara (CLA): Parte II – Ensaios no Túnel de Vento.* Revista Brasileira de Meteorologia, v.24, n.1, 87-99.

Sargison, J.E., Walker, G.J., Bond, V., Chevalier,G. 2004. *Experimental review of devices to artificially thicken wind tunnel boundary layer.* The University of Sydney, Sydney, Australia.

Versteeg, H. K., Malalasekera, W., 2007. *An Introduction to Computational Fluid Dynamics: The finite volume method.* Pearson Education, 2nd edition.

White, F. M., 2006. *Viscous Fluid Flow.* McGraw-Hill, 2006.

7. RESPONSIBILITY NOTICE

The authors are the only responsible for the printed material included in this paper.